

1 **JAST (Journal of Animal Science and Technology) TITLE PAGE**

2 **Upload this completed form to website with submission**

3

ARTICLE INFORMATION	Fill in information in each box below
Article Type	<a href="#">Research Article</a>
Article Title (within 20 words without abbreviations)	<a href="#">Comparison of estimating vegetation index for outdoor free-range pig production using convolutional neural networks</a>
Running Title (within 10 words)	<a href="#">Comparison of estimating vegetation index using different CNNs</a>
Author	<a href="#">Sang-Hyon OH [first author] 1, Hee-Mun Park [first author] 2, Jin-Hyun Park2</a>
Affiliation	<a href="#">1 Division of Animal Science, College of Agriculture and Life Science, Gyeongsang National University, Jinju 52725, Korea, Republic of</a> <a href="#">2 School of Mechatronics Engineering, Engineering College of Convergence Technology, Gyeongsang National University, Jinju 52725, Korea, Republic of</a>
ORCID (for more information, please visit <a href="https://orcid.org">https://orcid.org</a> )	<a href="https://orcid.org/0000-0002-9696-9638">Sang-Hyon OH (https://orcid.org/0000-0002-9696-9638)</a> <a href="https://orcid.org/0000-0001-5182-1739">Hee-Mun Park (https://orcid.org/0000-0001-5182-1739)</a> <a href="https://orcid.org/0000-0002-7966-0014">Jin-Hyun Park (https://orcid.org/0000-0002-7966-0014)</a>
Competing interests	<a href="#">No potential conflict of interest relevant to this article was reported.</a>
Funding sources State funding sources (grants, funding sources, equipment, and supplies). Include name and number of grant if available.	
Acknowledgements	
Availability of data and material	
Authors' contributions Please specify the authors' role using this form.	<a href="#">Conceptualization: OH SH, Park JH</a> <a href="#">Data curation: OH SH, Park HM, Park JH</a> <a href="#">Formal analysis: Park HM, Park JH</a> <a href="#">Methodology: OH SH, Park JH</a> <a href="#">Software: Park HM, Park JH</a> <a href="#">Validation: OH SH, Park HM, Park JH</a> <a href="#">Investigation: OH SH, Park HM, Park JH</a> <a href="#">Writing - original draft: OH SH, Park HM</a> <a href="#">Writing - review &amp; editing: OH SH, Park HM, Park JH</a>
Ethics approval and consent to participate	<a href="#">The present experiment was reviewed and approved by the Institutional Animal Care and Use Committee of North Carolina A&amp;T University (IACUC: 12-003.0).</a>

4

5 **CORRESPONDING AUTHOR CONTACT INFORMATION**

For the corresponding author (responsible for correspondence, proofreading, and reprints)	Fill in information in each box below
First name, middle initial, last name	<a href="#">Jin-Hyun Park</a>
Email address – this is where your proofs will be sent	<a href="mailto:uabut@gnu.ac.kr">uabut@gnu.ac.kr</a>

Secondary Email address	
Address	
Cell phone number	
Office phone number	
Fax number	

6

7

ACCEPTED

8 **Comparison of estimating vegetation index for outdoor free-range pig production using**  
9 **convolutional neural networks**

10

11 Sang-Hyon OH<sup>1†</sup>, Hee-Mun Park<sup>2†</sup> and Jin-Hyun Park<sup>2\*</sup>

12

13 <sup>1</sup>Division of Animal Science, College of Agriculture and Life Science, Gyeongsang National  
14 University, Jinju 52725, South Korea

15

16 <sup>2</sup>School of Mechatronics Engineering, Engineering College of Convergence Technology,  
17 Gyeongsang National University, Jinju 52725, South Korea

18

19 <sup>†</sup> Both authors contributed equally to this manuscript.

20 \*Corresponding author: [uabut@gnu.ac.kr](mailto:uabut@gnu.ac.kr)

21

22 Running Title: Comparison of estimating vegetation index using different CNNs

23

24 **ORCID**

25 **Sang-Hyon Oh** <https://orcid.org/0000-0002-9696-9638>

26 **Hee-Mun Park** <https://orcid.org/0000-0001-5182-1739>

27 **Jin-Hyun Park** <https://orcid.org/0000-0002-7966-0014>

28

29

30 **Title of the manuscript:** Comparison of estimating vegetation index for outdoor free-range  
31 pig production using convolutional neural networks

32

### 33 **ABSTRACT**

34 This study aims to predict the change in corn share according to the grazing of 20  
35 gestational sows in a mature corn field by taking images with a camera-equipped UAV. Deep  
36 learning based on convolutional neural networks (CNNs) has been verified for its performance  
37 in various areas. It has also demonstrated high recognition accuracy and detection time in  
38 agricultural applications such as pest and disease diagnosis and prediction. A large amount of  
39 data is required to train CNNs effectively. Still, since UAVs capture only a limited number of  
40 images, we propose a data augmentation method that can effectively increase data. And most  
41 occupancy prediction predicts occupancy by designing a CNN-based object detector for an  
42 image and counting the number of recognized objects or calculating the number of pixels  
43 occupied by an object. These methods require complex occupancy rate calculations; the  
44 accuracy depends on whether the object features of interest are visible in the image. However,  
45 in this study, CNN is not approached as a corn object detection and classification problem but  
46 as a function approximation and regression problem so that the occupancy rate of corn objects  
47 in an image can be represented as the CNN output. The proposed method effectively estimates  
48 occupancy for a limited number of cornfield photos, shows excellent prediction accuracy, and  
49 confirms the potential and scalability of deep learning.

50

51 **Keywords:** outdoor, pig, vegetation index, image analysis, convolutional neural network

52

53

### 54 **INTRODUCTION**

55 Pasture-based pig production is a common practice adopted in various countries,  
56 providing an opportunity for small-scale farmers to generate additional value within the context  
57 of corporate-driven swine industries. Iberico pork in Spain is a prime example, which has  
58 successfully demonstrated the potential benefits of Pasture-based pig production [1]. However,  
59 the expansion of this practice may lead to land degradation issues, warranting careful  
60 assessment and mitigation strategies. We presented two previous publications that have  
61 addressed the need for Pasture-based pig production and its associated land degradation  
62 problem [2, 3]. In this study, we focus on the crucial method of the land degradation assessment  
63 process: defining a suitable approach for measuring the extent of degradation in affected areas.

64 Digital image recognition technology is an image processing technology from computer  
65 vision. It has been applied in various areas of modern life, including security, the military,  
66 transportation, agriculture, medicine, and daily life [4,5,6]. However, it was difficult to  
67 recognize object features affected by camera settings, brightness around the object, and  
68 shadows. Utilizing multilayer artificial neural network algorithms in image recognition can  
69 allow more accurate object recognition even when there are changes to object features.  
70 However, this approach could have been impractical due to its high computation requirements.  
71 With the recent developments in semiconductor technologies, devices capable of parallel  
72 computing have been developed by integrating thousands of processing units into a single  
73 device, making it easier to implement algorithms with large amounts of computation. As a  
74 result, image recognition based on deep convolutional neural networks has also become  
75 practical technology [5-7].

76 Most yield predictions involve designing a Convolutional Neural Network (CNN)-based  
77 object detector for an image and predicting the yield or the occupancy by counting the number  
78 of detected objects or calculating the number of pixels occupied by the objects. However, these  
79 methods require multiple computational steps in addition to the detector, and their accuracy

80 depends heavily on whether the object features of interest are clearly visible in the image. For  
81 example, it is difficult to classify crops within images captured from high altitudes or wide  
82 areas. Moreover, deep learning-based image recognition in the agricultural domain requires a  
83 large amount of image data collected by experts in the field, and these images differ depending  
84 on the cultivation method, environment, and location [8-11]. Basic data augmentation involves  
85 applying various image processing techniques to preserve the characteristics of the original  
86 image while maintaining the diverse characteristics of the objects. These techniques vary from  
87 physically transforming images by randomly flipping, rotating, and cropping them to  
88 techniques that change the color or brightness of the images, such as inverting and channel  
89 mixing [8-13]. Two stages of processing are required to predict the yield or occupancy of a  
90 specific object. The first step is to classify specific objects in an image using a CNN, and the  
91 second step is to represent the occupancy rate of the classified objects based on the number of  
92 objects and the area they occupy. Calculating the degree of occupancy is a very cumbersome  
93 process. But another advantage of a CNN is that it also can be applied to function  
94 approximation and regression problems in addition to classifying objects [12,13]. Therefore, if  
95 a CNN is applied as a regression network, the occupancy rate of specific objects in an image  
96 can be represented by the network output without going through multiple calculation steps.

97 The objective of this study was to predict the occupancy rate of corn that has altered due  
98 to grazing by twenty gestating sows in a mature cornfield by capturing images with a camera-  
99 equipped UAV. A large amount of data is required to effectively train CNN-based deep learning,  
100 However, only a limited number of images were captured by the UAV so a data augmentation  
101 method that can effectively increase the data was proposed. Various CNNs were used as  
102 regression networks for comparison, and the applicability and scalability of deep learning were  
103 verified.

104

## 105 MATERIALS AND METHODS

### 106 Animal care

107 The present experiment was reviewed and approved by the Institutional Animal Care and Use  
108 Committee of North Carolina A&T University (IACUC: 12-003.0).

109

### 110 Study design and site

111 The images used for the analysis were taken at a swine unit located within the University Farm  
112 of North Carolina A&T State University (Greensboro, NC, USA; 36°4'16.63"N,  
113 79°43'33.02"E). A 50×100 m<sup>2</sup> grazing area was established for twenty pregnant sows that were  
114 allowed to graze pasture two weeks prior to their expected delivery date. The grazing area was  
115 planted with corn crops. The climate in this location is classified as a humid subtropical climate  
116 (Köppen climate classification), with hot and humid summers and mild winters. The average  
117 annual precipitation is around 107 cm. The sows were given access to slightly less than  
118 standard National Research Council balanced rations (2-3 kg/day) considering the consumption  
119 of corn in the pasture, but the water was provided *ad libitum*.

120

### 121 Data collection

122 A Phantom 2 Vision model UAV manufactured by DJI® with a quad-rotor system consisting of  
123 four propellers was used in this study. Including the camera, the maximum takeoff weight is  
124 1.3 kg, and it can fly for about 25 minutes using a 5,200 mAh lithium polymer battery. It has a  
125 remote-control range of up to 300 m and is equipped with a 1/2.3" high-resolution 14  
126 megapixels camera sensor with a fixed-focus wide-angle lens with a 120° FOV (Field of View)  
127 and a focal length of 28 mm. The UAV is equipped with an automatic flight control device, and  
128 a 2.4 GHz wireless remote controller was used for takeoff and landing as well as manual control

129 of the aircraft. Please refer to the research article by Oh et al. [2] for the detailed specifications  
130 of the UAV used in this study.

131 Ten aerial images were taken using the UAV from a height that allowed the entire grazing  
132 area to be captured in a single image. The image data were captured on days 2, 3, 4, 5, 7, 9, 10,  
133 11, 12, and 14 after releasing the gestating sows onto the cornfield from September 1<sup>st</sup> to  
134 September 13<sup>th</sup>, 2015, excluding days with rain. Also, the images were captured around 10:00  
135 AM without the need for additional lighting, and an effort was made to minimize the effect of  
136 shadows caused by the sun. In addition, a GPS attached to the UAV was used to attempt to  
137 maintain the same altitude and position for each image.

138

## 139 **Image Preprocessing**

### 140 *Convolutional Neural Network*

141 CNN is a multi-layered artificial neural network structure that is widely used for image  
142 recognition. It consists of a sequence of convolutional, non-linear, and pooling layers, followed  
143 by a fully connected layer that produces the final output. As the input image passes through the  
144 convolutional layers, specific features of the target object are revealed, and the final output is  
145 produced by the fully connected layer. The output layer can classify objects or produce  
146 regression values. Figure 1 represents the typical basic structure of CNN. The design of the  
147 layer structure can greatly affect the accuracy of the output and computation time. In particular,  
148 LeNet [5], developed by LeCun in the late 1990s, served as the basis for modern CNNs and  
149 had a significant impact on contemporary image recognition methods. CNNs convolve the  
150 entire image and intermediate feature maps to learn the various features of the objects in an  
151 image. As a result, CNNs make it relatively easy to find object features compared to traditional  
152 methods that require direct differentiation of objects. Additionally, CNNs can even identify  
153 features that are imperceptible to the human eye, resulting in very high recognition accuracy



154 [14]. CNNs continue to improve their performance in the field of image recognition, and the  
155 ImageNet Large Scale Visual Recognition Challenge (ILSVRC), which provides a common  
156 dataset for benchmarking machine learning and computer vision models, has further  
157 accelerated the development of CNN models through competition [15].

158 The first winner, AlexNet [16], expanded the input image size from  $32 \times 32$  in LeNet to  
159  $224 \times 224$ , increasing the model size, but solved the potential problem of overfitting by applying  
160 dropout layers and significantly improved its accuracy from 73.8% to 83.7% by applying the  
161 Rectified Linear Unit (ReLU) activation function to the ImageNet tests. VggNet [17] achieved  
162 remarkable results with an accuracy of 93.2% by increasing the number of convolutional filters  
163 and expanding the layer structure while unifying the convolution filter size to  $3 \times 3$  to reduce  
164 computation. However, there was no significant improvement compared to having 16 layers.  
165 GoogLeNet [6] improved the inefficient structure, and could model deeper than VggNet by  
166 using an inception module that included a  $1 \times 1$  convolution filter asymmetrically connected and  
167 layers that were not fully connected, resulting in a smaller model size and faster computation.

168 ResNet [7] recognized that designing a deeper layer structure to improve accuracy  
169 decreased performance and it achieved a higher performance by using residual learning.  
170 Residual learning can model with deeper layer structures by directly transmitting the next layer  
171 by skipping the adjacent convolutional layers without compromising the model's generalization  
172 performance. Therefore, CNNs have a significant impact on recognition accuracy and  
173 computation time depending on how the layer structure is modeled and can vary widely  
174 depending on the field of application, requiring extensive research under various conditions.

175

### 176 ***Image collection and preprocessing***

177 Images taken by the UAV are shown on days 3 and 10 after sows were released into the  
178 field in Figure 2. The images encompassing the entire cornfield have a resolution of

179 4,384×3,288 pixels, but the edges of the cornfield appear distorted into a fish-eye image.  
180 Fisheye images make the subject appear more prominent and can capture a wide range of  
181 backgrounds at the same time. However, the exact size cannot be recognized in such a distorted  
182 image because the object's size is distorted. Additionally, the camera mounted on the UAV  
183 could not consistently capture the cornfield at a fixed position and height, resulting in  
184 inconsistent left and right edges in the images, and images that included other objects outside  
185 of the cornfield. Therefore, image preprocessing was required so that the images only included  
186 the cornfield to accurately compare the corn occupancy rates of the images.

187 An example of image preprocessing steps for an image taken on day four after sows were  
188 released into a cornfield is illustrated in Figure 3. The original image on day four distorted into  
189 a fish-eye image is in Figure 3(a). The corrected result, as shown in Figure 3(b), is obtained by  
190 applying the correction method proposed by Scaramuzza [18], which is the best known in the  
191 field of computer vision, to the distorted fish-eye image. The method is computer vision's most  
192 representative and commonly used fisheye correction algorithm. The camera extrinsic and  
193 intrinsic parameters must be obtained to connect the 3D world coordinate points to the 2D  
194 image. World coordinate points are converted to camera coordinates using external parameters.  
195 Camera coordinates are mapped to the image plane using internal parameters. Still, a bird's eye  
196 view transformation is also required because the image is not captured at the center of the field.  
197 Fig. 3(c) shows an image containing only cornfields by transforming the bird's eye view and  
198 cropping the image. After completing the image preprocessing step, an example of 10 images  
199 is shown in Figure 4. The image generation was achieved by cutting the region of interest to  
200 3584×1792 pixels centered on the cornfield, ensuring that no other objects were in the image.

201

## 202 **Data Augmentation**

203 Much training data is required to train a deep learning network. Different corn object

204 images are needed to recognize and classify common corn objects according to the size, shape,  
205 illumination, and shadow state of corn objects. The ten transformed images were too few to be  
206 used as training and testing data for the deep learning networks, and the size of the corn objects  
207 was too small to extract sufficient features. Limited training data can lead to overfitting during  
208 network training, which can have a significant impact on performance. Fortunately, the  
209 resolution of the final images was much larger than the typical input resolution required for  
210 deep learning networks. A very high input resolution in a deep learning network increases the  
211 number of internal parameters of the network, resulting in a much longer training time, and  
212 increases the network processing time, resulting in learning and results processing difficulties.  
213 In addition, the accuracy of learning and prediction is affected by the very small size of the  
214 object (corn) in the image. To resolve this issue, the object in the image can be enlarged by  
215 cropping the network input resolution to be the size used for typical network training data. Data  
216 augmentation addresses the shortcomings of small training datasets by increasing the size of a  
217 training dataset by reflecting the characteristics of the data. Basic data augmentation can be  
218 performed on an image through various image processing techniques. A commonly used  
219 technique for data augmentation is to apply transformations that alter the physical form of the  
220 image, such as flipping the image horizontally or vertically, or rotating the image.

221 In this study, two different data augmentation techniques were performed for network  
222 training. First, the images were segmented to crop them to the appropriate size for a deep  
223 learning input image. Then the segmented images were randomly selected as raw training data,  
224 and data augmentation was performed by flipping and rotating the images.

225 Image segmentation is the process of dividing an image into smaller parts that are suitable  
226 for use as deep learning input images and increasing the amount of image data for deep learning  
227 network training. Figure 5 shows the image segmentation and augmentation process. The ten  
228 transformed images were divided into eight horizontal and four vertical sections to obtain 320

229 segmented images, which were used as training and testing data. Among them, 48 images were  
230 selected randomly as raw training images, and 6,912 training images were generated by  
231 flipping and rotating the images.

232 In the agricultural field, images acquired by UAVs are advantageous because they can  
233 undergo data augmentation by rotating the images. For recognizing objects in fields other than  
234 agriculture, small-angle rotation transformations are mainly applied. Therefore, the corn  
235 images captured by the UAV can still be used for analysis even if they are rotated 180 degrees.  
236 To increase the number of training images, 48 raw training images were horizontally flipped to  
237 create 96 images, and the resulting images were augmented by rotating them in 5-degree  
238 increments to produce 6,912 images. The 6912 training images generated by data augmentation  
239 are sufficient to train a CNN to predict the occupancy of a corn field.

240

## 241 **Convolutional Neural Network (CNN) Training**

### 242 ***Calculation of corn occupancy rate for training image***

243 This study aims to represent the process of cornfield degradation by gestation sows as  
244 numerical data using the degree of corn occupancy rate. The degree of corn occupancy rate  
245 needs to be known for each training image to train the deep learning network. To calculate the  
246 degree of occupancy of corn, corn objects are first labeled with three states (*CI*, *CD*, and *CS*) by  
247 corn field experts. *CI* represents the intact state where the corn has not been eaten or damaged  
248 by pigs, *CD* represents the state where the corn is damaged by pigs, and *CS* represents the state  
249 where pigs have eaten most the corn and only the cob remains. Table 1 shows an example of  
250 the boundary boxes labeled with three states for one of the 48 training images.

251 After labeling the corn state for any training image, the occupied area of the corn state is  
252 calculated.  $ACI$  is the area of corn labeled *CI*,  $ACD$  is the area of corn labeled *CD*, and  $ACS$  is  
253 the area of corn labeled *CS*. Therefore, the corn occupancy area ( $ACI_i$ ,  $ACD_i$ ,  $ACS_i$ ) according to

254 the corn state in the  $i^{\text{th}}$  image is calculated as in Equation (1), and the total corn occupancy rate  
 255 ( $ACT_i$ ) is represented as in Equation (2).

$$256 \quad ACT_i = \frac{\sum_{j=1}^{n_1} ACI_{ij}}{scale}, \quad ACD_i = \frac{\sum_{j=1}^{n_2} ACD_{ij}}{scale}, \quad ACS_i = \frac{\sum_{j=1}^{n_3} ACS_{ij}}{scale} \quad (1)$$

257 where,  $i$  is the number of the image,  $j$  is the number of  $CI$ ,  $CD$ , and  $CS$  in the image, and  
 258  $n_1$ ,  $n_2$ , and  $n_3$  represent the maximum number of  $CI$ ,  $CD$ , and  $CS$  in the image, and  $ACI_{ij}$ ,  
 259  $ACD_{ij}$ , and  $ACS_{ij}$  are the area of  $CI_{ij}$ ,  $CD_{ij}$ , and  $CS_{ij}$ , respectively. And the *scale* is set to  
 260 ensure that the occupancy rate of  $ACT_i$  does not exceed 1.

$$261 \quad ACT_i = w_1 \times ACI_i + w_2 \times ACD_i + w_3 \times ACS_i \quad (2)$$

262 where,  $w_1$ ,  $w_2$ , and  $w_3$  are weights for each corn state.

263 Table 2 shows an example of corn occupancy rates for the training images. The *scale* is  
 264 set to 11,000, and the weights [ $w_1, w_2, w_3$ ] are set to [1, 0.5, 0.2].

265

### 266 ***Convolutional Neural Network architecture and training***

267 CNN is the most widely used multi-layer structure for image recognition, along with  
 268 various models such as AlexNet, GoogLeNet, VggNet, and ResNet [6,7,15,16]. A CNN  
 269 structure using four CNNs was implemented to represent the degree of the corn occupancy rate  
 270 and to verify the potential of deep learning. CNNs have shown good results in image  
 271 classification and recognition and also can output regression values. Figure 6 shows a rough  
 272 CNN structure for outputting regression values. The input for the CNN is an image with  
 273  $448 \times 448$  pixels, and the output is the degree of corn occupancy rate for the input image as  $ACI_i$ ,  
 274  $ACD_i$ ,  $ACS_i$  and  $ACT_i$ . The network output applied a regression layer to produce regression  
 275 values and applied a ReLU layer to eliminate negative output values. The network was trained  
 276 with a dataset consisting of 6,912 images created by image augmentation and calculated data  
 277 on the degree of corn occupancy rate.

278

### 279 ***Proposed system***

280 The proposed system aimed to predict the degree of corn occupancy rate for corn images  
281 on a specific date after learning seven different types of CNN trained on a learning dataset  
282 created by data augmentation. Figure 8 illustrates the proposed system flow for a corn image  
283 taken on a specific date. A distorted fisheye image captured by the UAV on a specific date was  
284 corrected to  $3584 \times 1792$  pixels and divided into 32 ( $4 \times 8$ ) partitions, which were then  
285 sequentially fed into the CNNs. The CNNs learned from the sequentially inputted images,  
286 extracted the characteristics of the three corn states, and produced the degree of occupancy rate  
287 of the three corn states as outputs for each image. The occupancy rate of the entire cornfield on  
288 a specific date is  $ACT$ , which is the average value of  $ACT_i$  over 32 sequentially inputted image  
289 outputs, as shown in Equation (3). The  $ACI$ ,  $ACD$ , and  $ACS$  values in the network output can  
290 be used in Equation (2) to calculate the new occupancy rate by applying different weights  
291 depending on the state of corn.

$$292 \quad ACI = \sum_{i=1}^{32} ACI_i / 32, \quad ACD = \sum_{i=1}^{32} ACD_i / 32$$

293 (3)

$$294 \quad ACS = \sum_{i=1}^{32} ACS_i / 32, \quad ACT = \sum_{i=1}^{32} ACT_i / 32$$

295 where,  $ACI$ ,  $ACD$ , and  $ACS$  represent the occupancy rate of  $CI$ ,  $CD$  and  $CS$  for a corn image on  
296 a specific date, while  $ACT$  represents the overall occupancy rate of corn.

297

### 298 **RESULTS**

299 When there are a large number of images captured by a UAV, it is easier to apply a deep  
300 learning system, but when there is a very limited number of images, it is difficult to apply a

301 deep learning system. In addition, it is difficult to train deep learning when the captured images  
302 are distorted and not taken from the same location. The proposed system aimed to predict the  
303 occupancy rate of corn using a small number of distorted images captured by a UAV. Therefore,  
304 bird's-eye view images were used to correct the distorted fisheye images and extract corn field  
305 images containing no other object images. In addition, due to the lack of training images, the  
306 corn field images were divided into 32 parts and image augmentation was performed by  
307 randomly selecting raw training images and rotating and flipping them. Seven types of CNNs  
308 were trained using the 6,912 augmented training images, and the occupancy rate according to  
309 the corn states and the overall occupancy rate of corn on a specific date were predicted using  
310 the trained CNNs. AlexNet, GoogLeNet, Vgg16, Vgg19, ResNet50, and ResNet101 were  
311 applied to the structure of the CNN, and the applicability and scalability of deep learning were  
312 confirmed.

313 Figure 7 shows the degree of corn occupancy rate for all images. The CNN used a network  
314 provided by Matlab<sup>®</sup> [19] and the output network was configured to suit the proposed purpose.  
315 The same initial learning rate was set to 0.0001 to evaluate the performance of seven types of  
316 CNN. Adam Optimizer was used for learning, and network learning was performed with a  
317 maximum epoch of 500 and a mini-batch size of 32. The hardware used for the experiment was  
318 an Intel i9-12900 CPU and an NVIDIA RTX-A6000 graphics accelerator.

319 Table 3 shows the results of training the seven types of CNN. All networks were trained  
320 five times, and the performance evaluation index was obtained by averaging the values. The  
321 root mean square errors (RMSE) show that ResNet50 has the smallest learning error of the  
322 networks, while GoogLeNet has the largest. The network learning time varies depending on  
323 the size of the network, with AlexNet taking the shortest time and ResNet101 taking the longest  
324 time. Thus, AlexNet and the ResNet series were found to be advantageous in learning in terms

325 of RMSE and learning time.

326 Figures 9 to 12 indicate the occupancy rate according to the corn state and the total corn  
327 occupancy rate in order of date using the ten cornfield images input into the CNN. Overall, the  
328 graphs displayed similar trends. Figures 9(a)-12(a) show that the occupancy rate of undamaged  
329 corn (*ACT*) decreases gradually over time. Figures 9(b)-12(b) show that the occupancy rate of  
330 corn damaged by sows (*ACD*) sharply increases initially and then decreases rapidly from day  
331 4. Figures 9(c)-12(c) show that the occupancy rate of corn damaged by sows gnawing at the  
332 corn, leaving only a stump (*ACS*) also sharply increased until day 4 and then decreased  
333 gradually. Figures 9(d)-12(d) show that the overall occupancy rate of corn by date decreases  
334 exponentially over time across all networks. AlexNet, Vgg16, and Vgg19 show particularly  
335 good prediction accuracy compared to the other networks. GoogLeNet showed that the  
336 occupancy rates of *ACD* on day 3 and day 5 were slightly higher than on day 4, and the rates  
337 of *ACS* and *ACT* were slightly higher on days 11 and 12 compared to day 10. ResNet50 and  
338 ResNet101 generally showed good prediction accuracy, but their predictions were slightly  
339 higher on day 14. Overall, the CNNs demonstrated excellent prediction accuracy, confirming  
340 the potential and scalability of deep learning. The proposed method effectively estimated the  
341 occupancy rate of a limited number of cornfield photos, and there is a high potential for  
342 expanding it into other areas of livestock farming in the future.

343

## 344 **DISCUSSION**

345 Deep learning has been validated for its performance in various fields, and it has also  
346 demonstrated high recognition accuracy and detection time in agricultural applications, such  
347 as pest and disease diagnosis and prediction, fruit detection and maturity determination, and  
348 yield prediction [4-8,16,20,21]. In one agricultural application, Priyadharshini et al. [9]  
349 classified corn leaves into four states, three based on diseases that appear on corn leaves and



350 one normal state. They trained a modified version of LeNet [5] on the Plantvillage dataset and  
351 achieved a high accuracy of over 97%. Koirala et al. [10] suggested the Mango YOLO (You  
352 Only Look Once) network detects mangoes in real time and achieves excellent real-time  
353 performance with an F1 score of 0.97. Fu et al. [11] used the YOLOv4 network to accurately  
354 detect various sizes and shapes of bananas in harsh environments such as orchards. They  
355 demonstrated better detection speed and accuracy than tests performed on the YOLOv3  
356 network. Kitano et al. [12] used U-Net to predict the growth of corn at an early stage from  
357 images of corn fields taken by a UAV(Unmanned Air Vehicle). Mota-Delfin et al. [13] also  
358 used the YOLO method to effectively detect corn in cornfields with large numbers of weeds in  
359 the background and predict the yield. Oh et al. [2] trained a YOLOv4 network using a small  
360 number of images of cornfields and calculated the occupancy rate of cornfields by detecting  
361 corn objects.

362 The rationale behind choosing these specific models (AlexNet, GoogLeNet, VggNet,  
363 ResNet) was based on their well-established performance and effectiveness in various  
364 computer vision tasks. These models have been widely used and tested in different research  
365 and industrial applications, demonstrating state-of-the-art results in image recognition and  
366 classification tasks. Among the deep learning currently studied, the structures of CNNs to  
367 which regression can be applied represent the four network types tested in this study. Therefore,  
368 this experiment included the above four types and subtypes, and it is confirmed that deep  
369 learning shows robust performance not only for object classification tasks but also for  
370 regression. AlexNet was one of the pioneering deep learning models that gained significant  
371 attention after winning the ImageNet Large Scale Visual Recognition Challenge (ILSVRC) in  
372 2012. Its success was attributed to its deep architecture and the use of ReLU activation  
373 functions. GoogLeNet, also known as Inception, introduced the concept of inception modules,  
374 which allowed the network to capture features at multiple scales. This architecture proved to

375 be highly efficient and achieved outstanding performance on ILSVRC in 2014. VggNet, short  
376 for Visual Geometry Group Network, is known for its simple and uniform architecture with a  
377 deep stack of 3x3 convolutional layers. Despite its straightforward design, VggNet showed  
378 impressive results in ILSVRC 2014. ResNet (Residual Network) addressed the problem of  
379 vanishing gradients in very deep networks by introducing skip connections or residual blocks.  
380 This innovation enabled the successful training of extremely deep models, with ResNet  
381 becoming the winning model of ILSVRC 2015. Given their track record of success and the  
382 depth of their architectures, these models were chosen as they provided a strong foundation for  
383 comparison in this study of deep learning applicability and scalability.

384 In a pig grazing area, the decrease in the occupancy rate of undamaged corn over time  
385 could be attributed to several factors related to pig behavior. Pigs are known to forage and  
386 consume plants, including corn, as part of their diet. Over time, as pigs continue to graze in the  
387 area, they may consume or damage some of the undamaged corn plants, leading to a decrease  
388 in their occupancy rate. Pigs exhibit grazing behavior, preferring corn varieties, resulting in a  
389 higher rate of damage to corn plants, leading to a decline in their occupancy rate of intact corn.  
390 Pigs might cause physical damage to corn plants by trampling on them or rooting around the  
391 area. Such damage can hinder the growth and survival of corn plants, contributing to the  
392 decrease in their occupancy rate over time.

393 The sharp increase followed by a decrease in the occupancy rate of corn damaged by sows  
394 can be explained by several factors related to sow behavior. When sows are introduced to the  
395 grazing area, they might initially exhibit increased feeding activity and target the readily  
396 available and easily accessible corn plants. This initial feeding frenzy could lead to a sharp  
397 increase in the occupancy rate of damaged corn. Also, the grazing area was limited, the  
398 concentrated feeding activity of sows at the beginning could lead to a quick increase in the  
399 occupancy rate of damaged corn. In competition with other sows, if sows initially focus on

400 consuming only the intact corn ears, leaving behind the corn stalks, their main interest may  
401 shift elsewhere afterwards exploring other areas of the grazing field or shifting their focus to  
402 alternative food sources such as pellet feed. The combination of sow behavior mentioned above  
403 can lead to the observed pattern of an initial increase and subsequent decrease in the occupancy  
404 rate of corn damaged by sows, and this aligns with the results we have analyzed through images  
405 in this study.

406

## 407 **CONCLUSION**

408 Deep learning has proven its performance in various fields and has demonstrated high  
409 recognition accuracy and detection time in agricultural applications such as pest and disease  
410 diagnosis and prediction. Most yield predictions involve designing a CNN-based object  
411 detector for an image, counting the number of detected objects, or calculating the number of  
412 pixels occupied by objects to predict yield or occupancy. These methods require several  
413 computational steps besides a detector, and their accuracy strongly depends on whether the  
414 object features of interest are visible in the image. However, in addition to object detection and  
415 classification, CNNs can be applied to function approximation and regression problems.  
416 Therefore, if CNN is used as a regression network, the occupancy of a specific object in an  
417 image can be expressed as a network output without going through several calculation steps  
418 for object classification. This study applied the four most widely known networks (AlexNet,  
419 Vgg16, Vgg19, and GoogLeNet) as regression networks to predict the market share according  
420 to corn condition and total corn share in day order.

421 In conclusion, this study emphasizes the importance of accurately measuring and  
422 addressing land degradation concerns associated with pasture-based pig farming. The proposed  
423 methodology offers an effective means to evaluate the extent of land degradation with a limited  
424 number of cornfield photos showing excellent prediction accuracy, and confirms the potential

425 and scalability of deep learning. By taking proactive steps towards mitigating land degradation,  
426 the pasture-based pig farming sector can continue to thrive while preserving the environment  
427 and promoting socio-economic well-being.

428

429 **CONFLICT OF INTEREST**

430 We certify that there is no conflict of interest with any financial organization regarding the  
431 material discussed in the manuscript.

432

433

ACCEPTED

434 **REFERENCES**


- 435 1. Szyndler-Nędza M, Nowicki J, MaŁOpolska M. The production system of high quality pork  
436 products – an example. *Ann. Warsaw Univ. of Life Sci. – SGGW, Anim. Sci.* 2019;58(2):  
437 181–198.
- 438 2. Oh S, Park H, Park J. Estimating vegetation index for outdoor free-range pig production  
439 using YOLO. *Journal of Animal Science and Technology.* 2023;65(3): 638-651.
- 440 3. Oh S, Park H, Jung Y, Park J. 2023. Estimating vegetation index for outdoor free-range  
441 pig production. *Korean Journal of Agricultural Science.* 2023;50: 141-153.
- 442 4. Voulodimos A, Doulamis N, Bebis G, Stathaki T. Recent developments in deep learning for  
443 engineering applications. *Computational intelligence and neuroscience,* 2018; 8141259.
- 444 5. Krizhevsky A, Sutskever I, Hinton GE. Imagenet classification with deep convolutional  
445 neural networks. *Communications of the ACM.* 2017;60(6): 84-90.
- 446 6. Zou Z, Chen K, Shi Z, Guo Y, Ye J. Object detection in 20 years: A survey. *Proceedings of*  
447 *the IEEE.* 2023;111(3): 257-276.
- 448 7. Simonyan K, Zisserman A. Very deep convolutional networks for large-scale image  
449 recognition. *3rd International Conference on Learning Representations.*  
450 2015;arXiv:1409.1556.
- 451 8. Alibabaei K, Gaspar PD, Lima TM, Campos RM, Girão I, Monteiro J, Lopes CM. A Review  
452 of the Challenges of Using Deep Learning Algorithms to Support Decision-Making in  
453 Agricultural Activities. *Remote Sensing.* 2022;14(3): 638.
- 454 9. Priyadharshini RA, Selvaraj A, Madakannu A. Maize leaf disease classification using deep  
455 convolutional neural networks. *Neural Computing and Applications,* 2019;31(12): 8887-  
456 8895.
- 457 10. Koirala A, Walsh KB, Wang Z, McCarthy C. Deep learning for real-time fruit detection and  
458 orchard fruit load estimation: Benchmarking of ‘MangoYOLO’. *Precision Agriculture.*  
459 2019;20(6): 1107-1135.
- 460 11. Fu L, Duan J, Zou X, Lin J, Zhao L, Li J, Yang Z. Fast and accurate detection of banana  
461 fruits in complex background orchards. *IEEE Access.* 2020;8: 196835-196846.
- 462 12. Kitano BT, Mendes CCT, Geus AR, Oliveira HC, Souza JR. Corn plant counting using deep

- 463 learning and UAV images. *IEEE Geoscience and Remote Sensing Letters*. 2019. doi:  
464 10.1109/LGRS.2019.2930549.
- 465 13. Mota-Delfin C, López-Canteñs GJ, López-Cruz IL, Romantchik-Kriuchkova E, Olguín-  
466 Rojas JC. Detection and Counting of Corn Plants in the Presence of Weeds with  
467 Convolutional Neural Networks. *Remote Sensing*. 2022;14(19): 4892.
- 468 14. Shorten C, Khoshgoftaar TM. A survey on image data augmentation for deep learning.  
469 *Journal of big data*. 2019;6(1): 1-48.
- 470 15. Taylor L, Nitschke G. Improving deep learning with generic data augmentation. in 2018  
471 IEEE Symposium Series on Computational Intelligence (SSCI). 2018;arXiv:1708.06020
- 472 16. Lecun Y, Bottou L, Bengio Y, Haffner P. Gradient-based learning applied to document  
473 recognition. *Proceedings of the IEEE*. 1998;86(11): 2278-2324.
- 474 17. Wang X. Improving Bag-of-Deep-Visual-Words model via combining deep features with  
475 feature difference vectors. *IEEE Access*. 2022;10: 35824-35834.
- 476 18. Scaramuzza D, Martinelli A, Siegwart R. A flexible technique for accurate omnidirectional  
477 camera calibration and structure from motion. *Fourth IEEE International Conference on*  
478 *Computer Vision Systems (ICVS'06)*, New York, NY, USA, 2006;45.
- 479 19. The Math Works, Inc. MATLAB. R2021a, The Math Works, Inc., 2020. Computer Software.  
480 [www.mathworks.com](http://www.mathworks.com)
- 481 20. Szegedy C, Liu W, Jia Y, Sermanet P, Reed S, Anguelov D, Erhan D, Vanhoucke V,  
482 Rabinovich A. Going deeper with convolutions. *Proceedings of the IEEE conference on*  
483 *computer vision and pattern recognition*. 2015;arXiv:1409.4842.
- 484 21. He K, Zhang X, Ren S, Sun J. Deep residual learning for image recognition. *Proceedings*  
485 *of the IEEE conference on computer vision and pattern recognition*.  
486 2016;arXiv:1512.03385.

487

488

**Table 1. Image label**

<b>Label</b>	<b>Color</b>	<b>Corn description</b>	<b>Sample</b>
<i>CI</i>	Blue	Intact corn	
<i>CD</i>	Yellow	Damaged corn	
<i>CS</i>	Red	Corn with stubble	

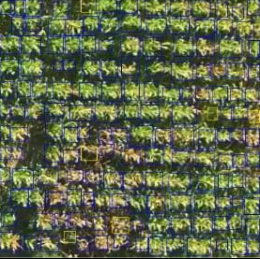
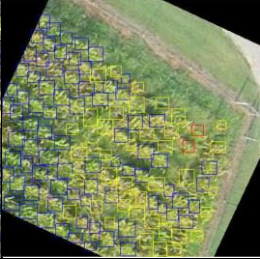
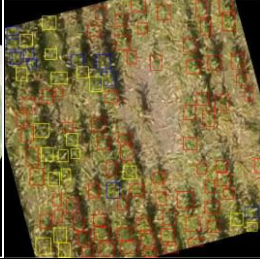

489

490

ACCEPTED

491

492 **Table 2. The occupancy rate of corn**

Sample Images				
$ACI_i$	0.975	0.369	0.036	0
$ACD_i$	0.026	0.164	0.080	0
$ACS_i$	0	0.007	0.288	0.005
$ACT_i$	0.988	0.452	0.134	0.001

493  $ACI_i$  : The occupancy rate of intact corn;  $ACD_i$  : The occupancy rate of damaged corn  
494 corn;  $ACS_i$  : The occupancy rate of corn with stubble;  $ACT_i$  : The occupancy rate of corn in  
495 all conditions

496

497

498



499 **Table 3. Training results**

Network(CNN)	RMSE	Training Time	Training Performance
<b>AlexNet</b>	0.16	74 min. 48 sec.	Very good
<b>GoogLeNet</b>	0.19	107 min. 16 sec.	Little good
<b>VggNet16</b>	0.14	355 min. 11 sec.	Good
<b>VggNet19</b>	0.14	414 min. 32 sec.	Good
<b>ResNet18</b>	0.14	88 min. 41 sec.	Very good
<b>ResNet50</b>	0.05	345 min. 45 sec.	Very good
<b>ResNet101</b>	0.07	623 min. 37 sec.	Good

500

501

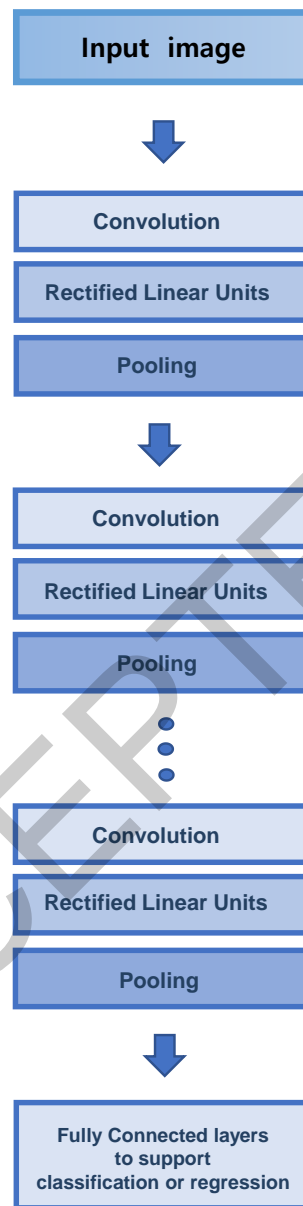
502

503

ACCEPTED

504

505



506

507 Figure 1. Structure of CNN

508

509



(a) Day 3



(b) Day 10

Figure 2. Examples of images taken by the UAV

510

511

512

ACCEPTED



513 (a) Distorted image

(b) Undistorted image

514 (c) Bird's eye view and cropping

515 Figure 3. Example of image correction.

516

ACCEPTED

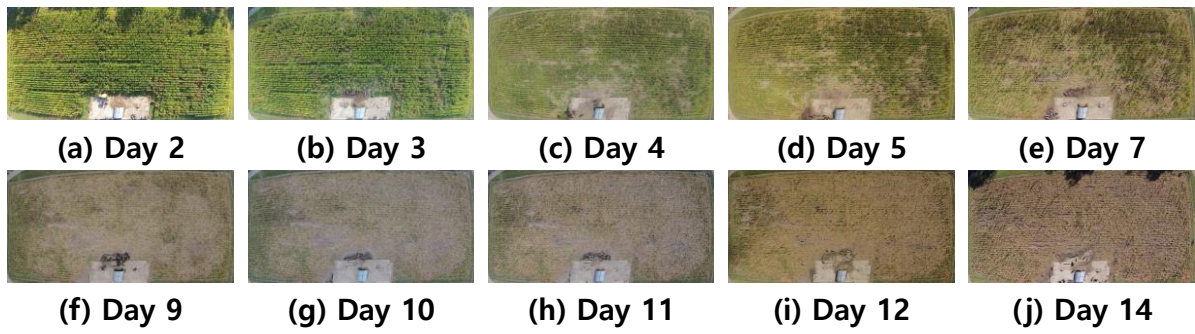


Figure 3. Images after pre-processing.

---

517  
518  
519

ACCEPTED

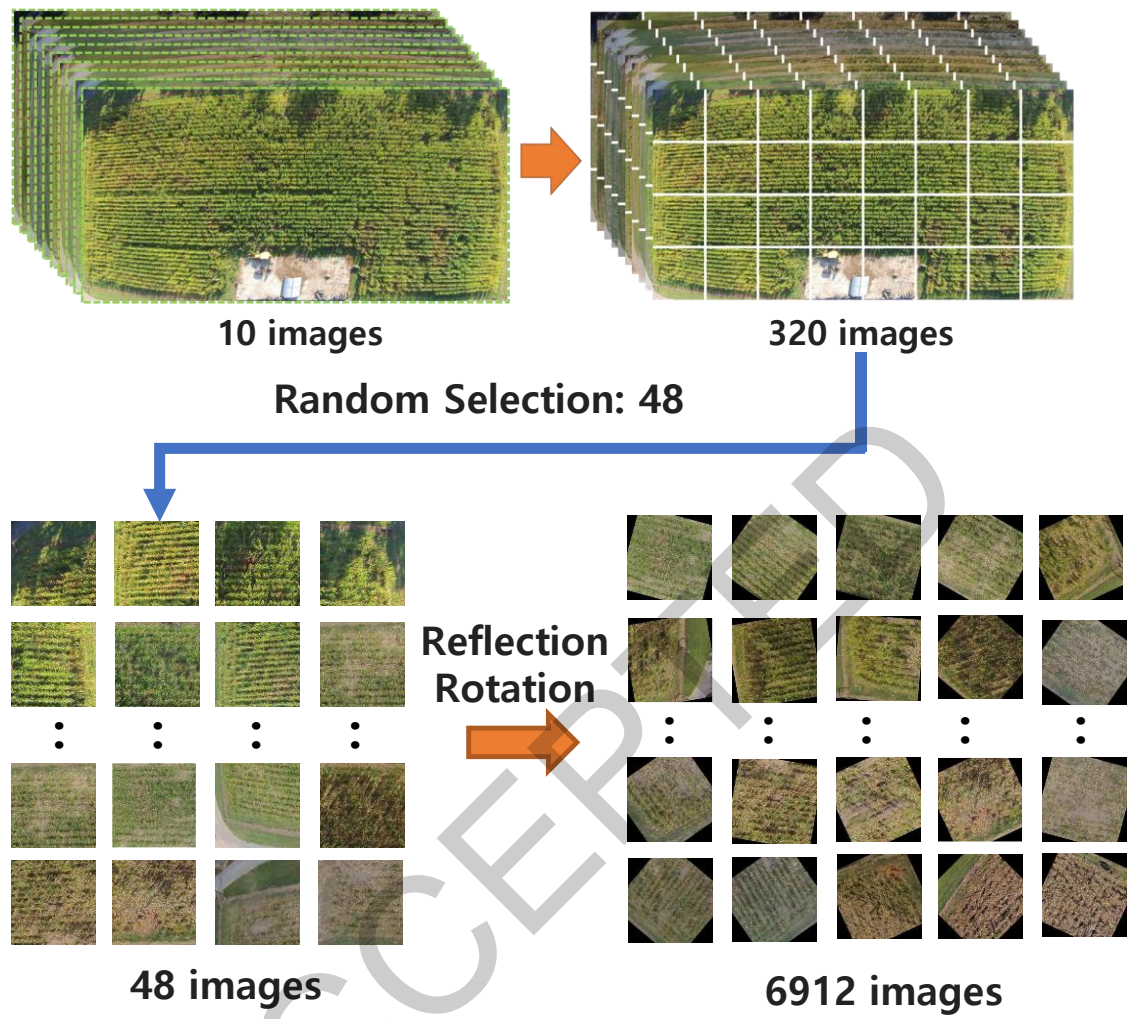
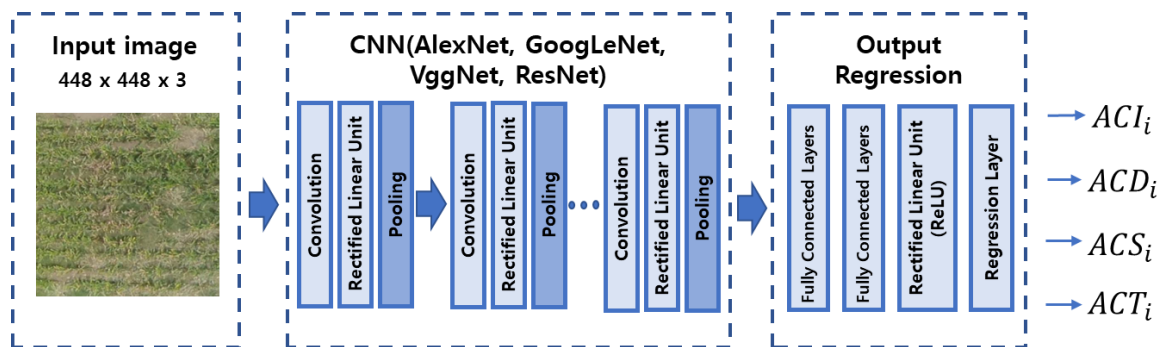


Figure 5. Data augmentation

524



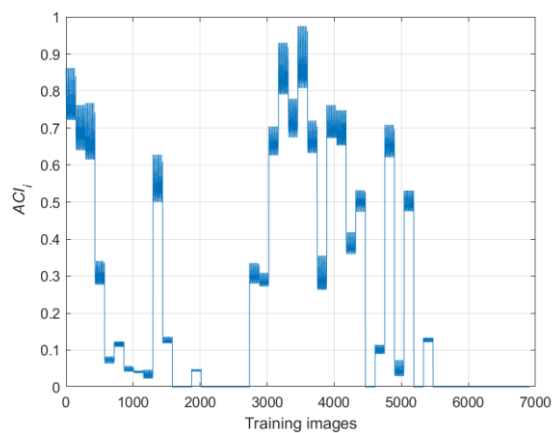
525

526

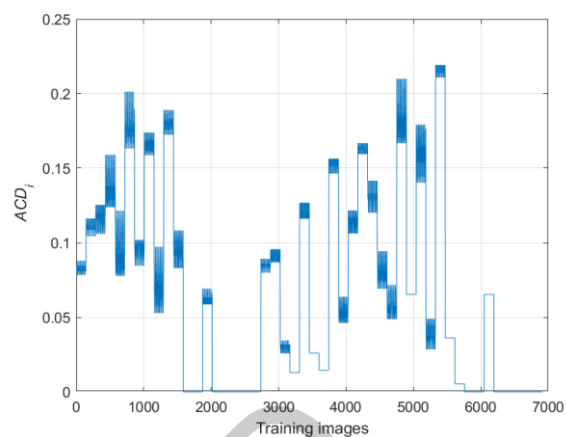
Figure 6. The CNN structure for regression

527

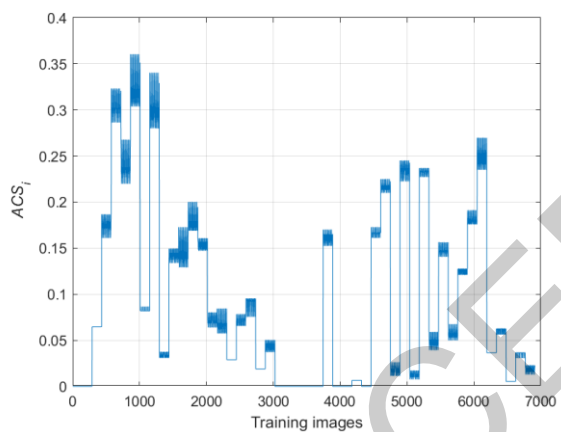
ACCEPTED



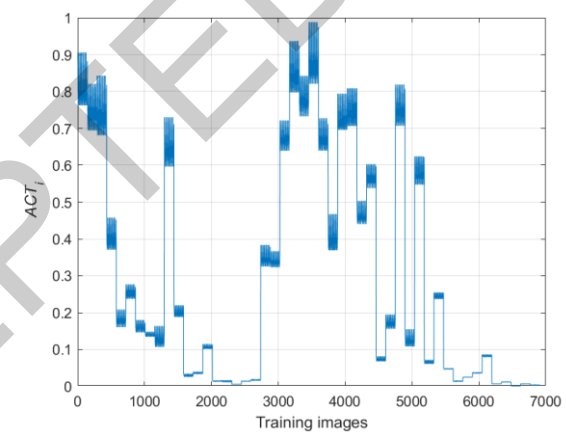
(a) The case of intact corn



(b) The case of damaged corn



(c) The case of corn with stubble



(d) The occupancy rate of corn

Figure 7. The degree of corn coverage in the training data



531

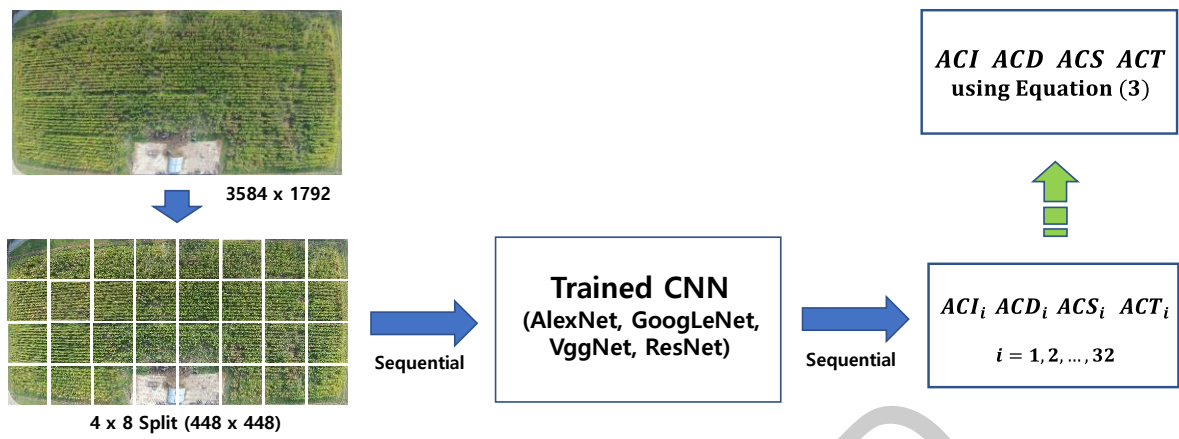


Figure 8. System configuration

532

533

534

ACCEPTED

535

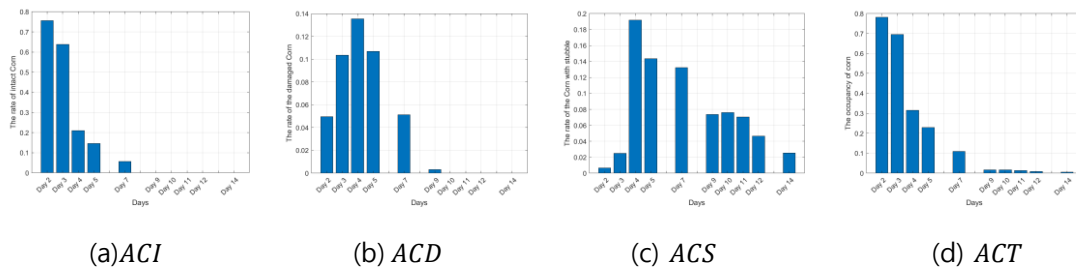


Figure 9. The occupancy rate of corn by date(AlexNet)

536

537

ACCEPTED

538

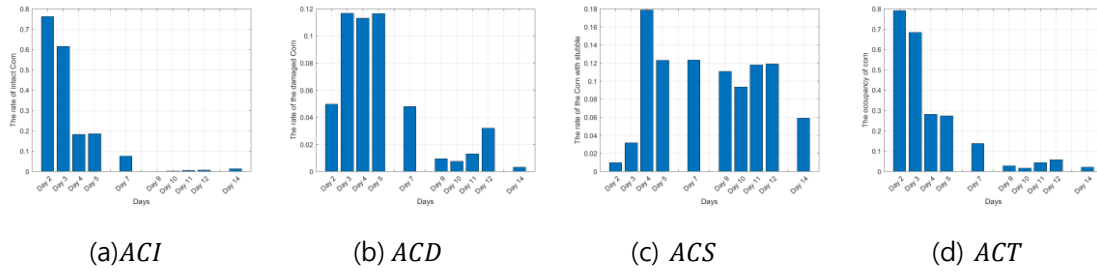


Figure 10. The occupancy rate of corn by date (GoogLeNet)

539

540

ACCEPTED

541

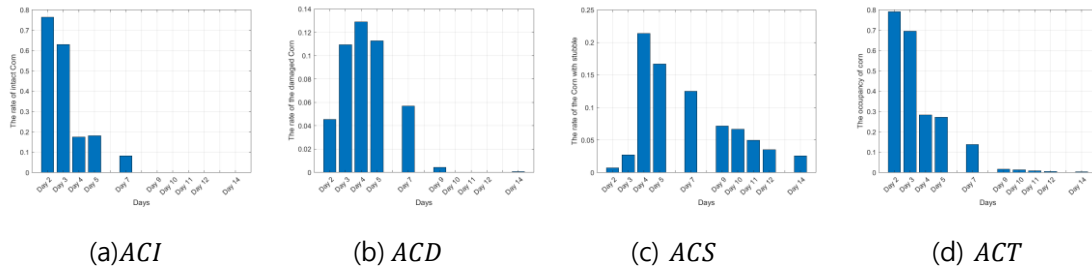


Figure 11. The occupancy rate of corn by date (Vgg16)

542

543

ACCEPTED

544

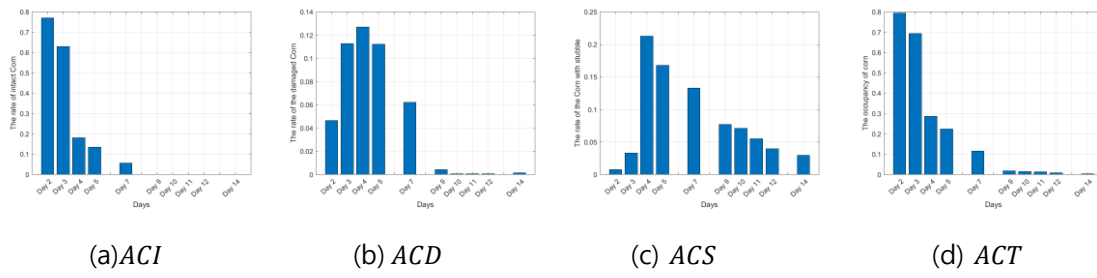


Figure 12. The degree of occupancy of corn by date(Vgg19)

545

546

ACCEPTED

547

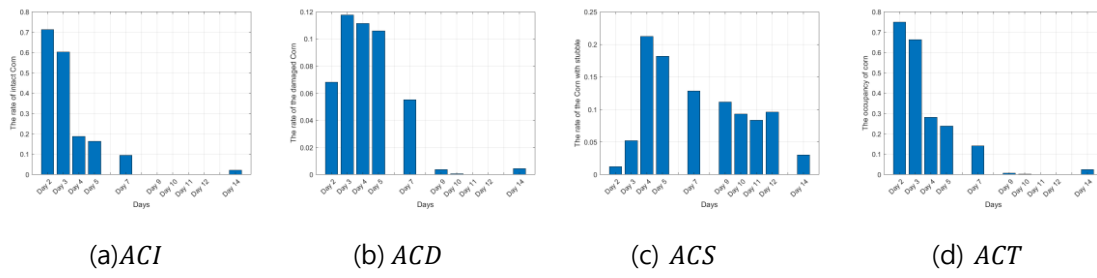


Figure 13. The degree of occupancy of corn by date(ResNet50)

548

549

ACCEPTED

550

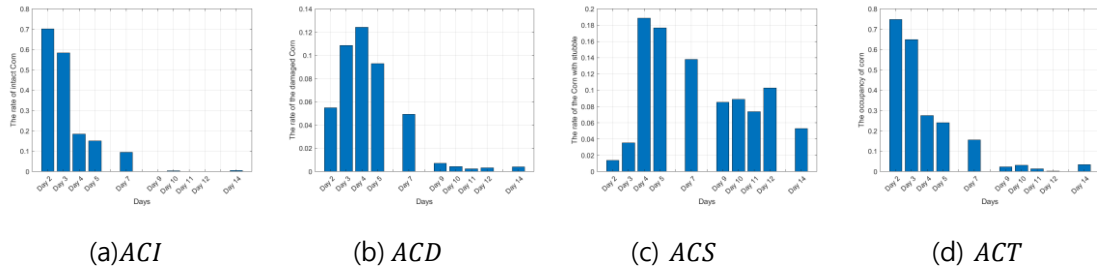


Figure 14. The degree of occupancy of corn by date(ResNet101)

551

552

ACCEPTED